Probabilistic investigation of sensitivities of advanced test-analysis model correlation methods

Elizabeth J. Bergman [a], Matthew S. Allen [a,*], Daniel C. Kammer [a], Randall L. Mayes [b]

[a] *Department of Engineering Physics, University of Wisconsin, Madison, WI 53706, USA*
[b] *Sandia National Laboratories[1], PO Box 5800, Albuquerque, NM 87185, USA*

ARTICLE INFO

ABSTRACT

The industry standard method used to validate finite element models involves correlation of test and analysis mode shapes using reduced Test-Analysis Models (TAMs). Some organizations even require this model validation approach. Considerable effort is required to choose sensor locations and to create a suitable TAM so that the test and analysis mode shapes will be orthogonal to within the required tolerance. This work uses a probabilistic framework to understand and quantify the effect of small errors in the test mode shapes on test-analysis orthogonality. Using the proposed framework, test-orthogonality is a probabilistic metric and the problem becomes one of choosing sensor placement and TAM generation techniques that assure that the orthogonality has a high probability of being within an acceptable range if the model is correct, even though the test measurements are contaminated with random errors. A simple analytical metric is derived that is shown to give a good estimate of the sensitivity of a TAM to errors in the test mode shapes for a certain noise model. These ideas are then applied to a generic satellite system, using TAMs generated by the Static, Modal and Improved Reduced System (IRS) reduction methods. Experimental errors are simulated for a set of mode shapes and Monte Carlo simulation is used to estimate the probability that the orthogonality metric exceeds a threshold due to experimental error alone. For the satellite system considered here, the orthogonality calculation is highly sensitive to experimental errors, so a set of noisy mode shapes has a small probability of passing the orthogonality criteria for some of the TAMs. A number of sensor placement techniques are used in this study, and the comparison reveals that, for this system, the Modal TAM is twice as sensitive to errors on the test mode shapes when it is created on a sensor set optimized for the Static TAM rather than one that was optimized specifically for the Modal TAM. These findings are evaluated in light of previously published studies of TAM sensitivity, and special attention is given to Gordis's theory, which suggest that TAM sensitivity is related to the natural frequencies of the structure when all measurement points are fixed. Some aspects of TAM sensitivity are problem dependent, so this one work cannot achieve a conclusive ranking of all of the available methodologies. Instead, this work focuses on presenting a set of tools and a probabilistic framework that can be used to correctly quantify TAM sensitivity and demonstrating the approach for one dynamic system and for a particular probabilistic model for the errors contaminating the test mode shapes.

---

1. Introduction

Finite element models have been used successfully for many years to predict the response of aerospace structures to their environmental loads. In order to ensure that critical predictions are accurate, each finite element model (FEM) must be experimentally validated, typically by comparing FEM modal parameters with those extracted from modal tests. This process has been called test/analysis correlation. Frequencies are compared directly, while the agreement between the mode shapes is most often evaluated by quantifying the orthogonality and cross-orthogonality of the modes. One can never measure at each node of the FEM, so a reduced representation, called a test-analysis model (TAM) is generated and the orthogonality of the modes is computed with respect to the TAM mass matrix [1]. Past experience has revealed that orthogonality is a good indicator of a valid FEM model, one which can be used confidently in coupled-loads analysis [2]. The use of these metrics, and the required values for test/analysis correlation, are dictated by agencies such as NASA [3] and the United States Air Force [1]. For example, the US Air Force requires test/analysis frequency errors less than or equal to 3.0%, cross-generalized mass values greater than 0.95, and coupling terms between modes of less than 0.10 in test-orthogonality and test-FEM cross-orthogonality (see [1], Sec. 5.12.3.10).

Many model reduction techniques have been developed, but the one that has been used the longest, and perhaps trusted the most, is the static or Guyan reduction [4]. However, there are cases where it does not provide accurate representations of the FEM, such as solid rocket motor applications [5]. Furthermore, it is sometimes very difficult to find a sensor set that is small enough to be practical, yet that still results in a good static TAM. This provided incentive for the development of a series of advanced TAM techniques, using Modal [6], Hybrid [7] and SEREP [8] reductions, which exactly predict the target modes, and the IRS TAM [9], which improves on the static TAM by approximating the inertia terms that are neglected in the static reduction.

While it is accepted that these advanced reduction techniques more accurately predict the FEM modal parameters and greatly improve orthogonality when the test mode shapes are equal to the FEM mode shapes, some works have found them to be more sensitive to FEM/test errors than Guyan reduction. Sensitivity produces larger off-diagonal terms in the orthogonality computations, and this sensitivity is thought to be a fault of the TAM rather than a meaningful indication of mismatch between the test results and the FEM. This is undesirable, not only from the analyst's point of view, but also from the test engineer's perspective, where the success of the test is based on minimizing the size of these terms. A few works have investigated TAM sensitivity using both simulated and actual experimental mode shapes. Chung [10] compared the Static, IRS, Modal, and Hybrid TAMs for three different systems, using real modal test data with the sensor locations optimized for the static reduction. He concluded that overall, the Static TAM performed the best, but the differences between the cross orthogonality terms for all of the methods were small for all three of the systems that he considered. Freed and Flanigan [11] investigated the same four TAMs for two different systems. The first system used simulated test data based on a modified FEM representation of a simple spacecraft. They placed sensors based on "kinetic energy and mode shape observability" [11] and found that the Hybrid and Modal TAM representations were the most sensitive to errors. Their second example employed real test data from the Titan dual payload, where the Hybrid TAM was observed to be the most robust, followed by the Static, IRS and then Modal TAMs. Avitable et. al. [12] compared Static, IRS, MAC [13], SEREP, and Hybrid TAM approaches. They used both simulated and real test data for a 2-bay truss. In the case of simulated experimental data, they found that the SEREP and Hybrid TAMs produced better orthogonality results than the Static TAM for large sensor sets, and significantly better results for reduced sets. For real test data, SEREP, Hybrid, and Static TAMs gave similar orthogonality results for large sensor sets, but the Static TAM was significantly worse for small sensor sets. Matsumura [14] compared the Static TAM with XORviaGDOP , which can be viewed as an extension to SEREP, observing that the latter was slightly more sensitive than the Static TAM, although the comparison was not pursued in detail.

All of the studies just cited used the same sensor set for each TAM, a sensor set that was usually chosen for the Static TAM, but each reduction procedure demands its own optimally placed sensor set. The Modal TAM requires that the target modes partitioned to the sensor set are as linearly independent as possible, as can be obtained using Effective Independence (EfI) [15] to place the sensors. The static reduction requires that the target modes be independent in a mass weighted sense. The studies just cited might have obtained artificially high sensitivity for the Modal TAM if the sensor set they employed was optimized for a different TAM. This work explores this issue using state of the art sensor placement techniques for each TAM, and also by comparing the performance of the Static and Modal TAMs on various sensor sets.

The most significant limitation of the previous works is that they employed a deterministic approach, computing the orthogonality of the test modes with respect to the TAM once, for a single set of test data, but the test mode shapes can be expected to vary significantly if the measurements are repeated so they should be modeled as random variables. In many of the studies cited previously, differences between the TAMs were small, so it was difficult to tell whether the differences were statistically significant. The key contribution of this work is that it uses a probabilistic framework to explore the question of TAM sensitivity to test errors, allowing one to quantify the sensitivity of each TAM in a meaningful way. Only one other work has taken a probabilistic view [14], but it was limited to the cross-orthogonality, a particular Gaussian noise model, and was focused on the XORviaGDOP TAM [14]. This work presents a procedure whereby the performance of the TAMs can be quantified probabilistically using Monte Carlo simulation. The problem is also treated analytically, resulting in a metric that can be used to estimate the sensitivity of the test-orthogonality to mode shape errors. Using a probabilistic approach, this work demonstrates that when sensitivity to errors is important, passing or failing the orthogonality criteria may be purely a matter of random chance. Failure to recognize this could cause significant

frustration for both experimentalists and analysts. If the experimentalists find that their initial test modes do not satisfy test-orthogonality, they are likely to invest extra time and effort in the test, perhaps adjusting boundary conditions, modifying modal parameter identification, checking sensor orientations, etc... This adds to the cost of the test, but would add little value if the initial test modes failed test-orthogonality only because of small, inevitable errors. Likewise, if an analyst encounters a model that has failed to meet validation criteria due to an overly sensitive TAM, they may:

- reject an FE model that is accurate to within the resolution of the test measurements,
- needlessly update an FEM model to recreate the random noise pattern observed in a particular test,
- make numerous perturbations to the TAM procedure, sensor set, or FEM model in an effort to pass the validation criteria, achieving little more than a random set of perturbations that passes the orthogonality metric for a given set of noise contaminated mode shapes and
- falsely conclude that an inadequate model is valid because it correlates well with a particular test.

   It is important to quantify the effect of measurement errors on test-orthogonality so that these scenarios can be avoided.
   The probabilistic framework proposed here is demonstrated by applying it to simulated measurements from a satellite system. A set of FEM target modes are corrupted with uniform random errors to simulate measurement errors, then the orthogonality of the noisy modes is computed with respect to four different TAMs, each of which was created with its own optimal sensor set. A Monte Carlo simulation is used to estimate the probability distributions for the average and maximum off-diagonal terms in the orthogonality. Both the examples and theoretical development presented here presume that the FEM is an accurate representation of the test hardware, so any mismatch between the FEM and test mode shapes is attributed to test errors. One would hope that the TAMs would indicate that the model is correlated in this situation, but the example shows that the probability of failing to meet test-orthogonality criteria may be high, even if the FEM is accurate and the errors in the test mode shapes are relatively small. Because of space limitations, only this one satellite system is considered, so the question of which TAM is best cannot be conclusively answered. However, the framework presented here can be used to understand the issues involved with TAM sensitivity and test/FEM correlation and to develop remedies.
   This paper is organized as follows. Section 2 summarizes existing methods and derives a metric to quantify TAM sensitivity using the probabilistic framework. The specific TAM generation and sensor placement methods that are used here are reviewed in Appendix A, as well as a new TAM generation method, the Inverse TAM, which is presented in Section A.1.4 and a new sensor placement method, the Condition number algorithm, which is presented in Section A.2.3. Section 3 describes the satellite model studied here and the pre-test correlation based on the perfect FEM model. Section 4 presents the mode shape error model and the results of the Monte Carlo simulation for each TAM method, and compares the results with the analytical predictions. Conclusions are presented in Section 5.

2. Theoretical development

2.1. Background

   Because the test mode shapes can never be measured at all of the nodes in a finite element model, one must either expand the test mode shapes to the FEM nodes or reduce the FEM to the test nodes before orthogonality can be computed. The latter approach is the focus of this work. The reduced FEM model is called a Test-Analysis Model (TAM). Using this paradigm, model correlation involves at least two stages. In the first stage a set of target modes is identified, a TAM model is created and a series of metrics are used to determine how well the TAM represents the FEM model. We shall denote the FEM target mode shapes partitioned to the sensor degrees of freedom as φ_{FEM}, the reduced mass matrix $\tilde{\mathbf{M}}_{\text{TAM}}$, and the target mode shapes calculated using the reduced mass and stiffness matrices φ_{TAM}. The metrics used to measure TAM/FEM correlation are orthogonality,

$$\mathbf{O} = \varphi_{\text{FEM}}^{\text{T}} \tilde{\mathbf{M}}_{\text{TAM}} \varphi_{\text{FEM}} \tag{1}$$

cross orthogonality,

$$\mathbf{CO} = \varphi_{\text{FEM}}^{\text{T}} \tilde{\mathbf{M}}_{\text{TAM}} \varphi_{\text{TAM}} \tag{2}$$

and comparison of the TAM and FEM natural frequencies

$$f_{\text{error}} = \frac{f_{\text{FEM}} - f_{\text{TAM}}}{f_{\text{FEM}}} \times 100 \tag{3}$$

Once an acceptable TAM has been created, one may proceed to test-analysis model correlation and then to updating. The TAM mass matrix is used to compute the orthogonality using Eqs. (1) and (2), only now between the test, φ_{test}, and FEM, φ_{FEM}, mode shapes. In all of the following, the term "orthogonality" and the symbols $\mathbf{O}$ and $\mathbf{CO}$ will be used to describe both TAM/FEM and Test/FEM orthogonality, as is typically done in the literature; it is clear from the context whether the TAM and FEM or the Test and FEM are being compared. Note that damping is not considered in traditional model correlation methods, so real mode vectors must be estimated from the test; this could be a concern if the structure in

question is very heavily damped or if one is concerned with high-fidelity modeling of damping, but these issues will not be considered here.

Most test-analysis models can be derived from the eigenvalue problem for the ith mode shape and frequency, partitioned into two sets of degrees of freedom. The degrees of freedom that will be retained are called the "a-set" and hence the corresponding matrices have a subscript of "a", while the omitted degrees of freedom are denoted as the "o-set" (subscript "o"). The partitioned eigenvalue problem can be written as follows:

$$-\omega_i^2 \begin{bmatrix} \mathbf{M}_{aa} & \mathbf{M}_{ao} \\ \mathbf{M}_{oa} & \mathbf{M}_{oo} \end{bmatrix} \begin{Bmatrix} \boldsymbol{\varphi}_{ai} \\ \boldsymbol{\varphi}_{oi} \end{Bmatrix} + \begin{bmatrix} \mathbf{K}_{aa} & \mathbf{K}_{ao} \\ \mathbf{K}_{oa} & \mathbf{K}_{oo} \end{bmatrix} \begin{Bmatrix} \boldsymbol{\varphi}_{ai} \\ \boldsymbol{\varphi}_{oi} \end{Bmatrix} = 0 \tag{4}$$

One can obtain the well-known dynamic reduction equation by extracting the lower partition and solving for at the o-set degrees of freedom from the a-set motion resulting in the following:

$$\boldsymbol{\varphi}_{oi} = -(\mathbf{K}_{oo} - \omega_i^2 \mathbf{M}_{oo})^{-1}(\mathbf{K}_{oa} - \omega_i^2 \mathbf{M}_{oa})\boldsymbol{\varphi}_{ai} \tag{5}$$

Dynamic reduction is theoretically exact, but the solution for the o-set is dependent on the frequency of the mode under consideration, so a reduced model obtained from dynamic reduction would have frequency dependent mass and stiffness matrices. To avoid this undesirable result, a number of alternatives have been proposed, four of which are utilized in this work: the static or Guyan TAM [4], the Improved Reduced System (IRS) TAM [9], the Modal TAM [5,6], and a new modal TAM named the Inverse TAM. The existing TAMs are reviewed in the Appendix in Sections A.1.1–A.1.3. The new Inverse TAM is presented in Section A.1.4.

Gordis [16] noted that one can think of these TAMs as an approximation to the dynamic reduction equation above, which depends on inverting the matrix

$$(\mathbf{K}_{oo} - \omega_i^2 \mathbf{M}_{oo}) \tag{6}$$

This matrix is ill-conditioned when ω_i^2 is near any of the eigenvalues of the $\mathbf{K}_{oo}$, $\mathbf{M}_{oo}$ system. The natural frequencies of the $\mathbf{K}_{oo}$, $\mathbf{M}_{oo}$ system are the natural frequencies that the system would have if it were were anchored at its a-set degrees of freedom. If those frequencies are near the natural frequencies of the actual system, then the dynamic reduction equation will be ill-conditioned. Physically, this means that the structure can have low frequency motion that is not observable on the a-set degrees of freedom, so the o-set motion cannot be determined from the a-set responses alone. Gordis noted this fact and suggested that the IRS TAM might greatly magnify errors in the test mode shapes if this is the case because the IRS TAM approximates the dynamic reduction equation. He suggested that one can test for sensitivity by computing the eigenvalues of the system with the a-set DOF restrained and see if the resulting frequencies are close to the frequencies of the actual system. Both Gordis [16], and Blelloch and Vold [17] seem to have extrapolated this theory to apply to any TAM that approximates the inertia terms, such as the Modal TAM. These ideas will be evaluated for a satellite system in Sections 3 and 4.

The accuracy of a test-analysis model clearly depends on which sensors are retained (the a-set); some sensor placement techniques have even been derived to be optimal for a certain TAM. Two existing sensor placement techniques, the Effective Independence (EfI) and modal kinetic energy techniques, are reviewed in the Appendix in Sections A.2.1 and A.2.2 respectively. A new sensor placement technique, dubbed the Condition number (C#) technique is presented in Section A.2.3.

2.2. Analytical evaluation of the effect of mode shape errors on test-analysis orthogonality

The same orthogonality equations are applied regardless of which TAM mass matrix and sensor locations are employed, so the following analysis applies to any of the methods just mentioned. Assuming that additive noise contaminates the test mode shapes, the test orthogonality of the i, jth term can be rewritten as follows where $\boldsymbol{\varphi}_i$ denotes the true test mode shape and $\mathbf{n}_i$ denotes errors that contaminate the ith mode shape.

$$O_{ij} = (\boldsymbol{\varphi}_i + \mathbf{n}_i)^{\mathrm{T}} \tilde{\mathbf{M}}(\boldsymbol{\varphi}_j + \mathbf{n}_j) \tag{7}$$

O_{ij} is the i, jth entry of the orthogonality matrix and $\tilde{\mathbf{M}}$ is the TAM mass matrix. This expression can be expanded into the following

$$O_{ij} = \boldsymbol{\varphi}_i^{\mathrm{T}} \tilde{\mathbf{M}} \boldsymbol{\varphi}_j + \boldsymbol{\varphi}_i^{\mathrm{T}} \tilde{\mathbf{M}} \mathbf{n}_j + \mathbf{n}_i^{\mathrm{T}} \tilde{\mathbf{M}} \boldsymbol{\varphi}_j + \mathbf{n}_i^{\mathrm{T}} \tilde{\mathbf{M}} \mathbf{n}_j. \tag{8}$$

Taking the expected value of Eq. (8), we can surmise that the mean of the orthogonality is equal to the true orthogonality (1st term) so long as:

- the error vectors $\mathbf{n}_i$ and $\mathbf{n}_j$ are zero mean (causing the expected values of the 2nd and 3rd terms to vanish) and
- each random variable in $\mathbf{n}_i$ is independent of each variable in $\mathbf{n}_j$ (causing the 4th term to vanish).

One way of interpreting Eq. (8) is to consider the 2nd and 3rd terms as random variables that are formed from linear combinations of the random variables comprising the noise vectors $\mathbf{n}_i$ and $\mathbf{n}_j$. Hence, if the noise on each random variable is

independent and identically distributed, then by the central limit theorem, the distribution of their sum becomes Gaussian as the number of sensor locations approaches infinity. The same is true for the 4th term, revealing that the noise on the orthogonality estimate is Gaussian under these circumstances. A Gaussian random variable is described completely by its mean and standard deviation [18]. The number of sensors is never really infinite in a real test, but this approximation can be quite accurate even with tens of sensors, and it is not uncommon for a modal test to employ a few hundred sensors in which case the approximation can be quite good.

The standard deviation σ_{Oij} of the i, jth term in the orthogonality matrix can be computed by subtracting the mean orthogonality μ_{ij} from O_{ij}, squaring the quantity and then finding its expected value.

$$\sigma_{Oij}^2 = E((O_{ij} - \mu_{ij})^2) \tag{9}$$

Under the assumptions stated above, the mean orthogonality is equal to the true orthogonality, so the first term in Eq. (8) cancels with μ_{ij} and there are only three terms to be squared. Each term is a scalar so six unique terms result and the expression becomes the following:

$$\sigma_{Oij}^2 = E[(\boldsymbol{\varphi}_i^T\tilde{\mathbf{M}}\mathbf{n}_j)^2 + (\mathbf{n}_i^T\tilde{\mathbf{M}}\boldsymbol{\varphi}_j)^2 + (\mathbf{n}_i^T\tilde{\mathbf{M}}\mathbf{n}_j)^2 + 2(\boldsymbol{\varphi}_i^T\tilde{\mathbf{M}}\mathbf{n}_j)(\mathbf{n}_i^T\tilde{\mathbf{M}}\boldsymbol{\varphi}_j) + 2(\boldsymbol{\varphi}_i^T\tilde{\mathbf{M}}\mathbf{n}_j)(\mathbf{n}_i^T\tilde{\mathbf{M}}\mathbf{n}_j) + 2(\mathbf{n}_i^T\tilde{\mathbf{M}}\mathbf{n}_j)(\mathbf{n}_i^T\tilde{\mathbf{M}}\boldsymbol{\varphi}_j)] \tag{10}$$

These terms simplify substantially if the noise is assumed to be uncorrelated and zero mean as was done above for the mean orthogonality. For example, the third term can be written as,

$$E[(\mathbf{n}_i^T\tilde{\mathbf{M}}\mathbf{n}_j)^2] = E[\sum_m\sum_n n_{mi}n_{nj}\tilde{M}_{mn}\sum_r\sum_s n_{ri}n_{sj}\tilde{M}_{rs}], \tag{11}$$

where $(\ )_m$ denotes the mth row of $(\ )$ and $(\ )_{mn}$ denotes the element at the mth row and nth column. Taking the summations to the outside and noting that, when the noise is uncorrelated and zero mean, the expectation of each term vanishes except for those for which $r=m$ and $s=n$, one obtains

$$E[\sum_m\sum_n n_{mi}^2 n_{nj}^2 \tilde{M}_{mn}^2] = \sum_m\sum_n \sigma_{\text{noise},mi}^2 \sigma_{\text{noise},nj}^2 \tilde{M}_{mn}^2 \tag{12}$$

where $\sigma_{\text{noise},mj}$ is the standard deviation of the noise for the jth mode and the mth sensor. The first and second terms can also be written in terms of the respective standard deviations. The situation is different for the fourth through sixth terms. For example, the fourth term can be written as,

$$E[2(\boldsymbol{\varphi}_i^T\tilde{\mathbf{M}}\mathbf{n}_j)(\mathbf{n}_i^T\tilde{\mathbf{M}}\boldsymbol{\varphi}_j)] = E(\sum_m\sum_n\sum_r\sum_s \phi_{mi}\tilde{M}_{mn}n_{nj}n_{ri}\tilde{M}_{rs}\phi_{sj}) \tag{13}$$

which reveals that this term vanishes if n_{ri} and n_{nj} are uncorrelated. The fifth and sixth terms likewise vanish, so one finally obtains the following expression for the standard deviation of the i, jth term of the test orthogonality matrix in terms of the standard deviation of the noise in each mode and at each sensor,

$$\sigma_{Oij} = \sqrt{\sum_m(\tilde{\mathbf{M}}\boldsymbol{\varphi}_i)_m^2\sigma_{\text{noise},mi}^2 + \sum_m(\tilde{\mathbf{M}}\boldsymbol{\varphi}_j)_m^2\sigma_{\text{noise},mj}^2 + \sum_m\sum_n\tilde{M}_{mn}^2\sigma_{\text{noise},mi}^2\sigma_{\text{noise},nj}^2}. \tag{14}$$

All of the terms are squared, so this reveals that TAMs which produce a TAM mass matrix with large elements, or large elements in $\tilde{\mathbf{M}}\boldsymbol{\varphi}_i$ will be most sensitive to noise. The expression can be easily implemented into a simple computational routine to compute the sensitivity of a TAM from its mass matrix and the target mode shapes. One should bear in mind that this equation was derived for a case where the noise contaminating the mode shapes is additive, zero mean and uncorrelated. Similar expressions could be derived for other noise models, such as multiplicative noise or correlated noise, but more complicated noise models quickly lead to a much more complicated expression, so the exercise might not produce much additional insight.

3. Pre-test correlation

3.1. Overview of satellite model

The proposed probabilistic framework was evaluated by applying it to the generic satellite shown in Fig. 1 The finite element model is comprised of 1191 nodes totaling 7146 degrees of freedom. The target modes chosen for this study are the first 18 elastic modes listed in Table 2; the system's six rigid body modes are not considered.

3.2. Sensor locations for satellite model

The sensor locations for the Static and IRS TAMS were found using the modal kinetic energy method. One would need about six-hundred sensors to capture 90% of the satellite's kinetic energy. This number of sensors would not be feasible in a real test, so the modal kinetic energy calculation was performed for each target mode independently and the six degrees of freedom with the largest kinetic energy were selected for each target mode. Only translational degrees of freedom were considered in this calculation. It was also discovered that the lumped masses had to be instrumented to provide an
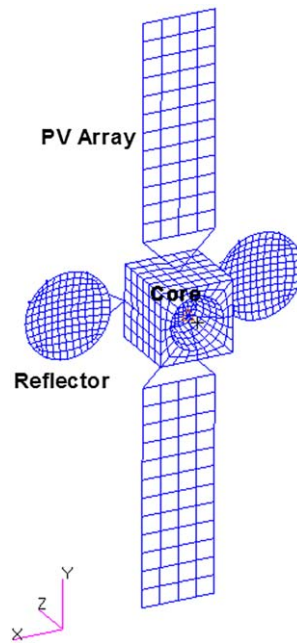
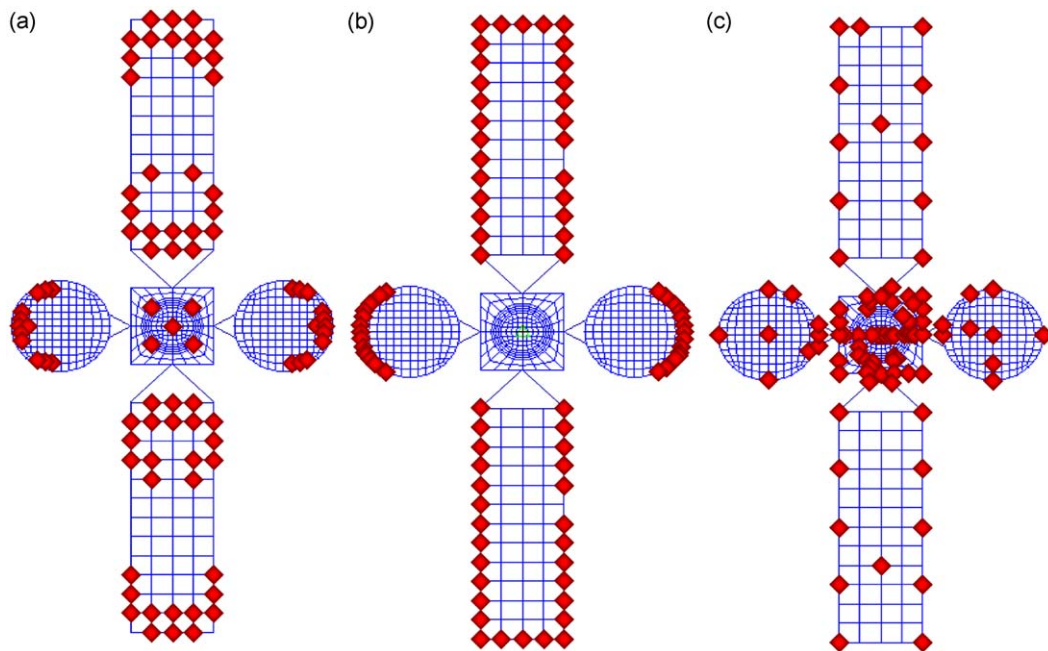**Fig. 1.** Generic Satellite with 7146 degrees of freedom.

Fig. 2. Static/IRS (a), Modal EFI (b) and Modal Condition Number TAM (c) sensor locations.

accurate Static TAM because they represent such a large portion of the mass of the structure. Therefore, these lumped masses were manually included in the KE sensor set used for the Static TAM. This resulted in a sensor set with 108 sensors to capture the 18 target modes. The Static/IRS TAM sensor locations, found using the KE method are shown in Fig. 2. Each diamond represents a sensor in the *X*, *Y*, or *Z* direction, or a combination of the three.

The Modal TAM EfI and C# sensor set locations are also shown in Fig. 2. Effective independence favors the edges of the satellite, and does not place any sensors on the satellite core. The C# sensor placement approach was initiated with a set of 26 sensors on the edges of the PV arrays and reflectors that were chosen to allow one to easily visualize the motion of

the satellite. The C# algorithm was then used to augment this set; the algorithm primarily selected additional sensors on the satellite core.

In order to examine Gordis' theory that the o-set dynamics determine TAM sensitivity [16], the a-set degrees of freedom, or sensor locations, determined using both the kinetic energy and Effective Independence sensor placement techniques, were constrained and the modes of the resulting constrained systems were computed. Table 1 lists the natural frequencies of the target modes of the actual system, the natural frequencies of the system with the sensor (a-set) DOF for the Static/IRS TAMs constrained, and those with the Modal EfI TAM sensors constrained. The lowest natural frequency of the system with the Static/IRS sensor locations constrained is 5 Hz higher than the highest target mode. On the other hand, the Modal EfI TAM a-set produces modes that are interspersed with the system natural frequencies. According to Gordis' theory discussed in Section 2.1, one would expect this Modal TAM to be highly sensitive to errors in the test mode shapes.

3.3. Pre-test TAM/FEM correlation results

Each sensor set provided acceptable TAM/FEM correlation when the perfect FEM modes were used. Table 2 displays the frequency error for the Static and IRS TAMs. The maximum frequency error for the Static TAM is approximately 2.3%, and the error is even smaller for the IRS TAM. As expected, the Modal TAMs reproduce the natural frequencies of the 18 target

Table 1
System natural frequencies and the natural frequencies when the sensor degrees of freedom (a-set) are constrained.

System Target Mode Nat. Freqs. (Hz)	Static/IRS Nat. Freqs. (Hz) with a-set constrained	Modal EfI Nat. Freqs. (Hz) with a-set constrained
0.31	16.84	0.37
0.63	16.84	1.18
0.80	17.45	1.88
1.79	17.45	2.65
2.72	17.76	3.19
2.83	17.76	5.91
3.49	19.56	17.35
3.68	19.56	17.35
3.99	23.85	17.61
4.24	25.03	17.64
5.91	27.14	17.76
6.41	27.14	17.76
7.46	31.33	19.33
7.48	31.33	19.35
9.61	31.34	21.52
9.71	31.34	21.52
11.75	35.03	21.92

Table 2
Static and IRS TAM frequency error.

| FEM target mode number	FEM Frequency (Hz)	Primary direction	Static TAM frequency error (%)	IRS TAM frequency error (%)
1	0.31	Z	0.00	0.00
2	0.63	X	0.00	−0.01
3	0.80	Z	0.00	0.00
4	1.79	X and Y	0.00	0.00
5	2.72	Z	−0.10	0.00
6	2.83	Z	−0.11	0.00
7	3.49	Z	−0.15	0.00
8	3.68	Z	−0.17	0.00
9	3.99	Z	−0.43	0.00
10	4.24	Z	−0.37	0.00
11	5.91	Y	−0.09	0.00
12	6.41	Y	−0.11	0.00
13	7.46	Z	−1.50	0.00
14	7.48	Z	−1.51	0.00
15	9.61	Z	−2.23	0.00
16	9.71	Z	−2.31	0.00
17	11.75	Z	−0.16	0.00
18	11.75	Z	−0.16	0.00
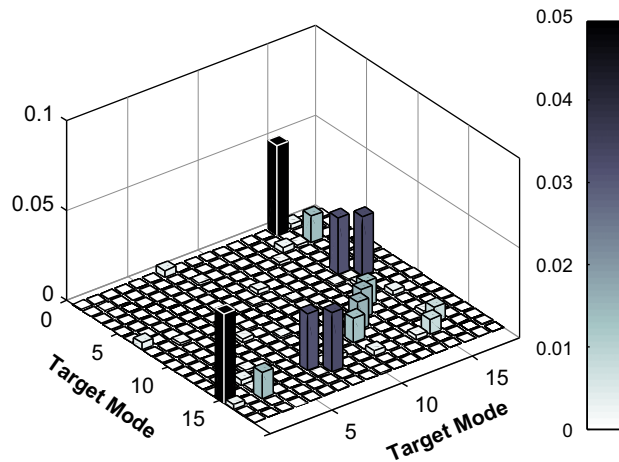
Fig. 3. FEM-TAM orthogonality matrix for the static TAM. The diagonal was removed by subtracting an identity matrix to aid in viewing the off-diagonal terms.

modes perfectly, and result in perfect orthogonality, so they are not included in Table 2. Fig. 3 displays the off-diagonal terms in the orthogonality matrix for the Static TAM. The maximum off-diagonal orthogonality and cross-orthogonality values for the Static TAM were 0.05 and 0.031, respectively, while the corresponding values for the IRS TAM were all less than 0.01.

4. Probabilistic study of test-analysis correlation for generic satellite model

4.1. Noise model

In practice, model updating and validation are complicated by the fact that experimental measurements are contaminated with both random noise and systematic errors. Some sources of measurement error include: errors in the positioning and alignment of the sensors, imperfect modal parameter extraction, sensor calibration inaccuracy, cross-axis sensitivity and electrical noise. These errors have not all been thoroughly quantified in the literature, yet there is increasing interest in doing so [19]. For example, a number of recent works have sought to estimate the variance of the modal parameters estimated by state of the art modal parameter estimation routines [20–22].

For the present study, experimentally measured mode shapes were simulated by adding uniformly distributed noise to each finite element mode shape. The simulated noise was created by adding a vector of uniformly distributed random numbers to each mode shape, scaled to 2% of the maximum value of that mode shape. This noise model was used because it assures that the noise on the mode shapes is bounded, but it results in the maximum entropy for a given set of bounds. Specifically, the rth simulated test mode vector was,

$$\boldsymbol{\varphi}_{\text{test},r} = \boldsymbol{\varphi}_{\text{FEM},r} + \mathbf{n}_r \tag{15}$$

$$\mathbf{n}_r = c_r \varepsilon \mathbf{u}_r \tag{16}$$

where $\boldsymbol{\varphi}_{\text{test},r}$, FEM target mode shape with added noise; $\boldsymbol{\varphi}_{\text{FEM},r}$, FEM target mode shape; $\mathbf{n}_r$, vector of noise added to FEM target mode shape; ε, noise level, in this study $\varepsilon = 0.02$; c_r, scaling factor, $c_r = \max(\boldsymbol{\varphi}_{\text{FEM},r})$; $\mathbf{u}_r$, vector of independent uniformly distributed random numbers between -1 and 1.

The actual noise profile obtained in a real experiment is much more complicated than that represented here, yet one would expect that the magnitude of the uncertainty in each element of an experimentally measured mode shape may be even greater than 2%. For example, accelerometer calibration factors are typically reported with a 95% confidence interval of $\pm 4\%$, so typical uncertainty due to calibration alone can be greater than the 2% uncertainty used here.

4.2. Results

The test-orthogonality, **O**, between the noise-contaminated mode shapes, was computed using each of the TAM mass matrices. The result found using the Static TAM mass matrix is displayed in Fig. 4 for one realization of the noise model. Comparing this with the orthogonality matrix computed using perfect mode shapes in Fig. 3, we observe that almost all of the off-diagonal terms have increased and a few exceed the US Air Force test-orthogonality criteria of $O_{ij} < 0.1$, $i \neq j$. This result represents the orthogonality matrix that might be obtained from a single test due to random test errors. The result
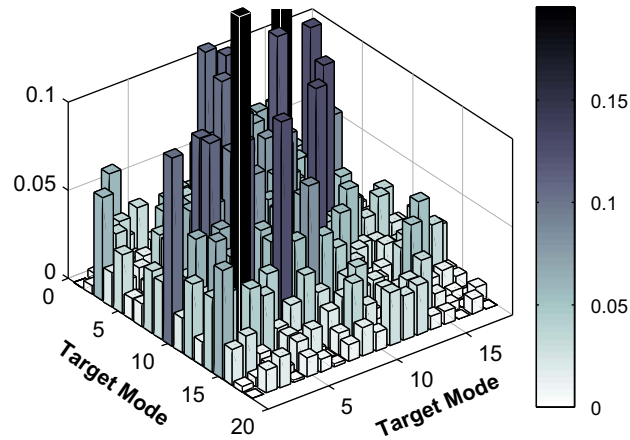
Fig. 4. Static TAM test-orthogonality matrix using simulated test mode shapes. The diagonal was removed by subtracting an identity matrix to aid in viewing the off-diagonal terms.
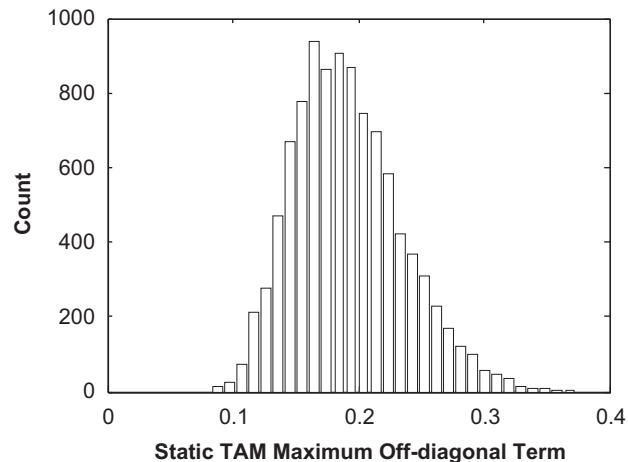

Fig. 5. Histogram of maximum off-diagonal term in static TAM test-orthogonality.

obtained in a given test depends on the specific value of the noise obtained in each mode shape coefficient, so one might pass or fail to pass the test-exit criteria, depending on the particular pattern of errors in the test mode shapes.

Because the orthogonality is a random variable, it must be described statistically. Perhaps the best way to do this is to compute the probability of passing or failing the orthogonality criteria given the assumed noise model. In order to do this, a Monte Carlo Simulation (MCS) was performed. The test-orthogonality calculation was repeated for 10,000 random noise profiles, and the maximum and average off-diagonal terms in the orthogonality computation were stored for each trial. Fig. 5 shows a histogram of the maximum off-diagonal terms obtained in the MCS. One can observe that the maximum off-diagonal term exceeds the Air Force validation criteria in most of the trials, so according to that criteria the FEM model would not be considered valid for most of the trials. A kernel density estimator [23] was used to estimate the probability of obtaining acceptable orthogonality, which was found to be $P(\max(O_{ij}) < 0.1) = 0.003$. This means that test personnel utilizing this TAM would have about a three in one-thousand probability of meeting the test exit criteria, depending on the specific errors obtained in the set of measured modes, or in other words, depending on random chance. Similar trends were observed for the cross-orthogonality.

A number of TAMs were studied and probability density functions (PDFs) of the MCS results were estimated for each using the kernel density estimator in [23]. Fig. 6 shows estimates of the PDFs of the maximum off-diagonal term in the test orthogonality calculation for the Static, IRS, Modal Effective Independence (EfI), Modal Condition Number (C#), and Inverse (C#) TAMs. As expected, the PDFs show that the probability of obtaining a maximum off-diagonal term of zero is small, because that requires that all of the off-diagonal terms be zero simultaneously. The probability of obtaining a passing maximum off-diagonal value (i.e. less than 0.1) is quite small for both the Static and IRS TAMs, so these TAMs would almost always erroneously indicate that the model is not correlated. On the other hand, the test mode shapes satisfy the
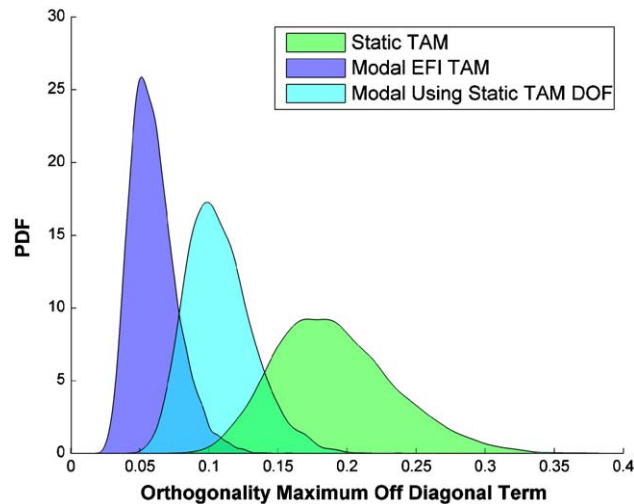
Fig. 6. Estimated probability density functions of maximum off-diagonal term in test-orthogonality matrix for Static, EFI Modal, Condition Number Modal, and Condition Number Inverse TAMs for the satellite system presented in Section 3.1.

Table 3
Test-orthogonality statistics for various TAMs and sensor placement schemes.

	Maximum orthogonality off-diagonal		Average orthogonality off-diagonal		Condition number of ϕ_a
	Mean	STD	Mean	STD	
Static	0.191	0.043	0.029	2.9E−03	14.446
IRS	0.758	0.069	0.244	2.8E−02	14.446
Modal EfI	0.060	0.017	0.008	7.0E−04	16.227
Modal on Static					
TAM Sensor Set	0.108	0.024	0.016	1.6E−03	14.446
Modal C# TAM Starting with Visualization Set (Fig. 6)	0.055	0.011	0.010	9.0E−04	3.759
Modal C# TAM Starting with 3 sensors with largest EfI	0.055	0.010	0.011	7.6E−04	6.317
Modal C# TAM Starting with 15 lumped masses	0.032	0.005	0.008	5.2E−04	2.334

orthogonality criteria most of the time when the Modal TAM is used. The Modal TAM gives similar results whether effective independence or the condition number approach is used for sensor placement. The PDF for the Inverse C# TAM overlays that of the Modal C# TAM, indicating that the two have similar sensitivity for this problem. One should bear in mind that the PDFs presented were estimated from the results of the Monte Carlo simulation, so they are not exact, but should be quite accurate for such a large number of MCS samples.

The MCS data is displayed numerically in Table 3, which lists the mean and standard deviation over the 10,000 MCS trials of the maximum off-diagonal terms for each TAM. (The mean of the maximum off-diagonal term corresponds to the centroid of the PDFs shown in Fig. 6.) PDFs of the average off-diagonal term were not shown graphically, but their mean and standard deviations are also given in Table 3. Comparing the statistics of the maximum and average off-diagonal terms, one finds that the average terms are an order of magnitude lower than the maximum terms. This was also observed in the individual noise-contaminated orthogonality results, one of which was shown in Fig. 4. Further investigation revealed that certain modes were often responsible for the large maximum off-diagonal terms. The most common offender was the coupling between modes 3 and 14, which also corresponds to the largest off-diagonal term in Fig. 4. Mode 3 involves anti-symmetric bending in the Z-direction; mode 14 primarily involves motion of the reflectors.

The statistics in Table 3 can be used to compare the different TAMs for this system. The ideal TAM is characterized by a low mean value, which indicates that the maximum or average orthogonality is small. The standard deviation should also be small, indicating that similar orthogonality results would be obtained for any realization of the random noise model. The results in Table 3 indicate the Modal TAM is clearly the least sensitive to errors for this system while the IRS TAM is the most sensitive. The orthogonality of the Modal TAM was found on two additional sensor sets, both of which were created using the Condition number algorithm. The first sensor set was obtained by starting with the 3 sensors possessing the highest effective independence, while the second started with the 15 lumped masses on the core of the satellite. The C# TAM discussed up until this point, and shown in Fig. 6, was created by starting with a 26 sensor visualization set, as

described in Section 3.2. These results show that the condition number sensor placement technique does generally result in a very robust TAM; all three TAMs based on the C# sensors passed the orthogonality criteria most of the time, but the results do show that the sensor set found by the C# algorithm depends heavily on the initial sensor set. The condition numbers shown in the table reveal that TAM robustness generally increased as the condition number decreased, but there are exceptions. For example, the IRS TAM had a slightly lower condition number than the Modal EfI TAM, yet it was much more sensitive to mode shape errors than the Modal EfI TAM. On the other hand, the most robust TAM in terms of the maximum off-diagonal term was a Modal C# TAM, and it had the smallest condition number of those investigated.

The method described in Section 2.2, which predicts the standard deviation of each term in the test orthogonality matrix, was applied to each of the TAMs used in this study. Note that the method in Section 2.2 predicts the standard deviation of a single off-diagonal term in the orthogonality matrix prior to any other processing. In contrast, the standard deviations listed in Table 3 were obtained by first finding the maximum or average of the absolute value of the orthogonality over all of the sensor locations and then computing the sample standard deviation of these quantities over 10,000 MCS trials. A more detailed analysis than that presented in Section 2.2, including the correlation between each term in the test-orthogonality matrix, would be required to predict the statistics shown in Table 3, so the standard deviation predicted by Eq. (14) is compared directly with the standard deviation computed from the MCS results for each of the terms in the test-orthogonality matrix. Table 4 shows this comparison, but for brevity the standard deviations are only compared for ijth element of the orthogonality matrix, where i and j are the indices of the element in the test-orthogonality with the largest standard deviation. The percent difference between the two is also shown. The analytical method based on Eq. (14) predicts the standard deviation very precisely for all of the TAMs except the Static and IRS TAMs.

Mode 3 was often coupled to other modes in the orthogonality calculation. Fig. 7 shows the shape of that mode, and the shape obtained after contaminating the mode shape at the sensor locations with simulated errors as discussed previously, and then expanding the shape to all of the nodes in the FEA model. Both the Static TAM and the Modal EfI TAM

Table 4
Test-orthogonality: predicted and actual standard deviations of O_{ij}.

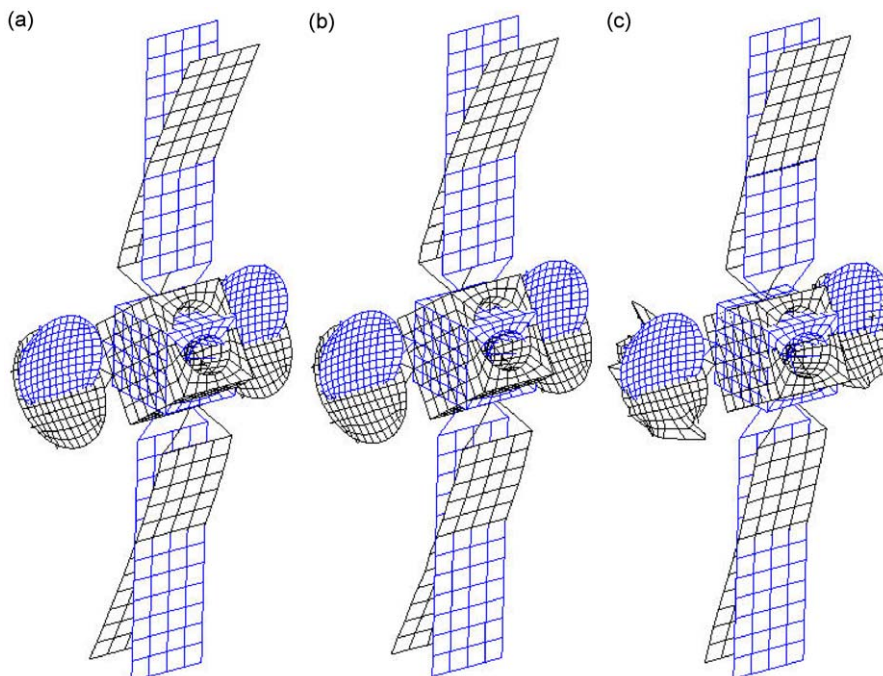| TAM	Pred. σ_{ij}	MCS σ_{ij}	% Error	i	j
Modal Efl	0.038	0.039	0.7	14	4
Static TAM	0.149	0.132	−11.5	3	14
Modal on Static					
TAM Sensor Set	0.075	0.071	−5.6	14	3
Modal C# TAM Starting with Visualization Set (Fig. 6)	0.027	0.027	0.4	9	4
IRS	12.490	0.418	−96.7	14	13

Fig. 7. Analytical mode shape 3 (a), noisy mode shape expanded using Modal EFI TAM (b), and noisy mode shape expanded using Static TAM (c).
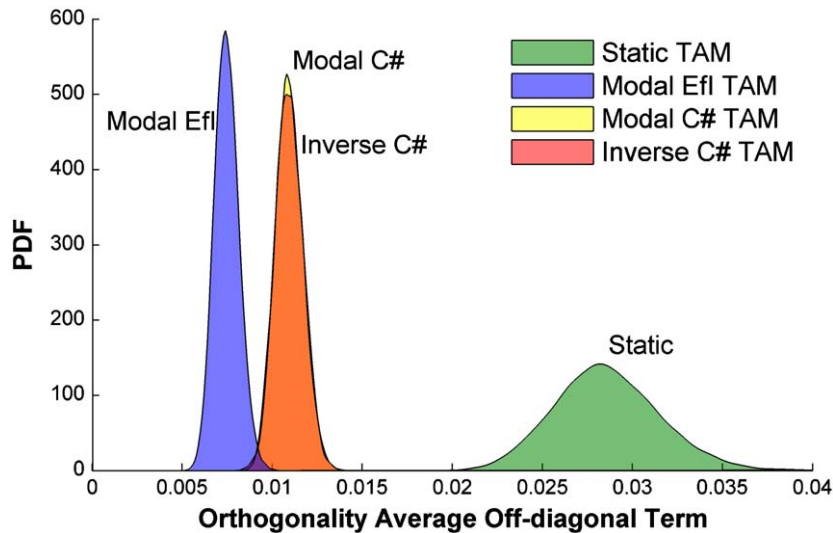
Fig. 8. Estimated probability density functions of maximum off-diagonal term in test-orthogonality matrix for Static, EfI Modal TAM and Modal TAM created using the Static TAM sensor locations.

transformation matrices were used in the expansion. The Static TAM produces artificially jagged reflector motion at many of the *o*-set degrees of freedom, indicating that it is sensitive to measurement noise. On the other hand, the modal TAM transformation gives a very good approximation of the *o*-set motion in spite of the noise on the *a*-set measurements.

As noted previously, different sensor placement techniques have been developed for use with the different TAM methods. The importance of the sensor locations was studied by creating another Modal TAM using the sensor locations that were optimized for the Static TAM. As noted previously, many of the previous comparisons of the Static and Modal TAMs have created both on the same sensor set, usually a sensor set that was optimized for the Static TAM. The PDF of the maximum off-diagonal term for this sub-optimal Modal TAM is shown in Fig. 8. The corresponding result for the previously described Static and Modal EfI TAMs are repeated for comparison. The Modal TAM is much more sensitive to mode s hape errors when implemented using the Static TAM sensor locations, although in this case it is still less sensitive than the Static TAM.

4.3. Discussion

It was noted that the US Air Force orthogonality criterion would have a small probability of being satisfied using either the Static or IRS TAMs for this system and number of sensors. This is of concern because the simulated experimental mode shapes are merely noise contaminated copies of the true mode shapes, so it would be a mistake to update the finite element model to better correlate with these mode shapes, but the orthogonality criteria would most likely indicate that this is necessary when these TAMs are used. Of course, the probability of passing is heavily dependent on the noise model. The noise model considered here corrupts the mode shapes at points with small motion most severely. This is often observed experimentally so it is not physically unrealistic, but it may explain the high sensitivity for this satellite whose massive core moved little. A multiplicative noise model was also considered, in which each element of each mode shape was contaminated by no more than 2% of its actual value. In that case the PDFs of the maximum off-diagonal term shifted left so that they were usually less than 0.1 for the Static TAM and all of the Modal TAMs, but the rankings between the methods were essentially the same. Likewise, with 5% uniform, multiplicative noise all of the TAMs pass the orthogonality criterion with high probability except for the Static TAM, which has about a 65% probability of passing. Future works should certainly seek to develop more accurate noise models, but in any event the procedure developed here can be employed to evaluate TAM sensitivity, no matter which noise model is considered to be most realistic for a particular scenario.

In Table 4, the standard deviations obtained from the Monte Carlo simulation were compared with those predicted using the formula developed in Section 2.2. It was noted that the formula did not agree very well with the MCS results for the Static and IRS TAMs. However, this discrepancy can be explained by the fact that when performing the MCS, the noise contaminated eigenvectors were re-normalized to make the diagonal terms of the test orthogonality unity, as is commonly done in practice. This renormalization was not considered in the analytical sensitivity analysis. The Static and IRS TAMS were very sensitive, so this normalization had a significant effect for them, while the diagonal terms for the modal TAMs were always near one, so the normalization did not change the noise level for those TAMs. It is also worth noting that

the predicted standard deviations in Table 4 follow the same rankings as the means of the maximum off diagonal term in Table 3, suggesting that Eq. (14) can be used to rank the TAMs or to develop a more robust sensor placement technique.

5. Conclusions

This work presented a stochastic framework that can be used to rigorously characterize the sensitivity of a test-analysis model to errors in the test mode shapes. Mode shape errors may arise due to imperfections in modal parameter extraction, sensor calibration errors, measurement noise, accelerometer cross-axis sensitivity, etc…. The analysis presented in Section 2.2 revealed that each term in the orthogonality matrix will tend toward a Gaussian distribution if the mode shape errors are independent and identically distributed, and those ideas were used to develop a metric that relates to the sensitivity of a TAM to mode shape errors. These ideas were validated using simulated measurements from a satellite. Errors in the test mode shapes were modeled as uniformly distributed random noise scaled to a small fraction of the maximum value of each mode shape. The system studied here exhibited considerable sensitivity for the number of target modes and sensors selected, which would cause the Static and IRS TAMs to have a small probability of passing the test-orthogonality criteria, even though the test mode shapes were contaminated with a relatively small level of noise. The sensitivity of the TAMs to the sensor placement technique was also explored, and it was observed that a Modal TAM created on the Static TAM sensor set was twice as sensitive as a Modal TAM created using Effective Independence to place sensors. A new sensor placement technique, dubbed the Condition number algorithm, was presented and found to reduce the sensitivity of the Modal TAM to mode shape errors for the satellite system studied here.

While only one system was considered here, the procedure developed here can be applied to virtually any system. One could also use this approach to define the criteria (e.g. number of sensors or target modes, etc…) under which model correlation is possible for the TAM of interest and a certain level of sensor noise. One could also develop an improved sensor placement algorithm based on the analytical orthogonality estimate presented here, which would provide a set of sensor locations that minimizes the TAM's sensitivity to errors in the test mode shapes. In doing so, it will be important to develop an accurate model for the measurement errors, and this will probably not be a trivial task, but considering the potential magnitude of the problem, it is a task that should certainly be pursued.

This study also investigated Gordis' theory [16] regarding TAM sensitivity, and demonstrated a case that contradicts the theory: the Modal TAM was not overly sensitive for this satellite, even though its constrained *a*-set natural frequencies were interspersed with the target modes natural frequencies (see Table 1).

The authors would like to emphasize that this study does not purport to determine definitely which TAM is the most sensitive. The performance of each TAM is probably dependent on the model, the number and character of the target modes selected, and the sensor locations. However, the approach presented here can be used to study sensitivity and TAM performance from a probabilistic viewpoint, and it is hoped that these methods will be employed to allow engineers to make more informed decisions regarding TAM sensitivity.

Appendix A. Review of TAM generation and sensor placement techniques

A.1. Test-analysis models (TAMs)

A.1.1. Static (Guyan) TAM

The Static TAM is the most common model reduction technique and is available in many commercial finite element codes. The Static TAM neglects the inertia terms and hence removes the dependency on frequency. The resulting static transformation is thus given by

$$\mathbf{T}_S = \begin{bmatrix} I \\ -\mathbf{K}_{oo}^{-1}\mathbf{K}_{oa} \end{bmatrix} \tag{17}$$

The statically reduced mass and stiffness matrices are then given, respectively, by

$$\tilde{\mathbf{M}}_S = \mathbf{T}_S^{\mathrm{T}}\mathbf{M}\mathbf{T}_S \tag{18}$$

$$\tilde{\mathbf{K}}_S = \mathbf{T}_S^{\mathrm{T}}\mathbf{K}\mathbf{T}_S \tag{19}$$

Each column of $\mathbf{T}_S$ represents the elastic deformation of the structure under a unit displacement of the corresponding *a*-set degree-of-freedom with all others constrained. These shapes are also referred to as constraint modes.

A.1.2. Improved reduced system (IRS) TAM

The Improved Reduced System (IRS) TAM [9] aims to improve upon the Static TAM by approximating the neglected inertia terms. The frequency dependent terms in Eq. (5) are approximated using the statically reduced mass and stiffness matrices.

$$\omega_i^2\{\boldsymbol{\varphi}_{ai}\} \approx \tilde{\mathbf{M}}_S^{-1}\tilde{\mathbf{K}}_S\{\boldsymbol{\varphi}_{ai}\} \tag{20}$$

The IRS transformation matrix can be written as the Static transformation matrix plus a correction term, $\mathbf{T}_i$.

$$\mathbf{T}_{\text{IRS}} = \mathbf{T}_S + \mathbf{T}_i \tag{21}$$

$$\mathbf{T}_i = -\begin{bmatrix} 0 & 0 \\ 0 & -\mathbf{K}_{oo}^{-1} \end{bmatrix} \begin{bmatrix} \mathbf{M}_{aa} & \mathbf{M}_{ao} \\ \mathbf{M}_{oa} & \mathbf{M}_{oo} \end{bmatrix} \begin{bmatrix} I \\ -\mathbf{K}_{oo}^{-1}\mathbf{K}_{oa} \end{bmatrix} \tilde{\mathbf{M}}_S^{-1} \tilde{\mathbf{K}}_S \tag{22}$$

The reduced mass and stiffness matrices, $\tilde{\mathbf{M}}_{\text{IRS}}$ and $\tilde{\mathbf{K}}_{\text{IRS}}$, are computed as in Eqs. (18) and (19).

A.1.3. Modal TAM

There are circumstances in which the Static TAM fails to accurately represent the dynamics of the full system because it neglects the mass associated with the o-set degrees of freedom. For instance, a solid rocket motor application [5] contained modes that were dominated by massive and soft propellant. The Static TAM neglected terms that were significant to the analysis and thus did not provide a good representation of the system. The modal TAM was developed to resolve this issue. The method uses the modal expansion equation for the target modes

$$\mathbf{x} = \boldsymbol{\varphi}\mathbf{q} \tag{23}$$

where $\boldsymbol{\varphi}$ represents the target modes, and $\mathbf{q}$ represents the generalized modal coordinates. This equation can be partitioned into the a-set and o-set degrees of freedom,

$$\begin{Bmatrix} \mathbf{x}_a \\ \mathbf{x}_o \end{Bmatrix} = \begin{bmatrix} \boldsymbol{\varphi}_a \\ \boldsymbol{\varphi}_o \end{bmatrix} \mathbf{q} \tag{24}$$

and one can then solve for the modal response vector $\mathbf{q}$,

$$\mathbf{q} = (\boldsymbol{\varphi}_a^{\text{T}}\boldsymbol{\varphi}_a)^{-1}\boldsymbol{\varphi}_a^{\text{T}}x_a \tag{25}$$

This requires that the matrix $(\boldsymbol{\varphi}_a^{\text{T}}\boldsymbol{\varphi}_a)$ be invertible, so the number of a-set degrees of freedom must be greater than or equal to the number of target modes and the target modes must be linearly independent when partitioned to the sensor locations. The transformation matrix for the Modal TAM is found by substituting Eq. (25) into the lower partition of Eq. (24), resulting in the following.

$$[\mathbf{T}_M] = \begin{bmatrix} I \\ \boldsymbol{\varphi}_o(\boldsymbol{\varphi}_a^{\text{T}}\boldsymbol{\varphi}_a)^{-1}\boldsymbol{\varphi}_a^{\text{T}} \end{bmatrix} \tag{26}$$

The reduced mass matrix $\tilde{\mathbf{M}}_M$ is computed in the usual way. The primary advantage of the Modal reduction method is that it is exact for the modes used in the reduction process, so the TAM/FEM correlation is always perfect.

A.1.4. Inverse TAM

The Inverse TAM was developed by Mayes during the course of this work, and is based upon the same principles as the Modal TAM. One advantage of the inverse TAM is that it can be created from the mode shapes directly, without the finite element mass matrix; this can greatly reduce the computational expense required to find an optimum sensor set. The Inverse TAM is derived from the orthogonality property of mass normalized mode shapes

$$\boldsymbol{\varphi}_a^{\text{T}}\tilde{\mathbf{M}}_{\text{IM}}\boldsymbol{\varphi}_a = \mathbf{I} \tag{27}$$

where $\boldsymbol{\varphi}_a$ represents the target mode shapes partitioned to the sensor locations and $\tilde{\mathbf{M}}_{\text{IM}}$ is the reduced Inverse TAM mass matrix. The Inverse TAM mass matrix is found by solving Eq. (27). Typically, $\boldsymbol{\varphi}_a$ is not a square matrix, so the pseudoinverse is employed. The resulting expression for $\tilde{\mathbf{M}}_{\text{IM}}$ is

$$\tilde{\mathbf{M}}_{\text{IM}} = (\boldsymbol{\varphi}_a^{\text{T}})^+ (\boldsymbol{\varphi}_a)^+ \tag{28}$$

where $(\ )^+$ denotes the Moore–Penrose pseudoinverse. The reduced mass matrix found using Eq. (28) is not full rank because there are generally more sensors than modes, but the method can be modified to create a full-rank TAM mass matrix if desired.

A.2. Sensor placement algorithms

Three techniques are used to generate sensor locations in this work: a modified version of modal kinetic energy (Section A.2.1), effective independence (Section A.2.2) and a new method (Section A.2.3) that seeks to minimize the condition number of the a-set modal matrix. The modal kinetic energy method is best suited for the Static and IRS TAMs, while the other methods are best suited for the Modal TAM and Inverse TAMs.

A.2.1. Modified modal kinetic energy (KE)

Modal kinetic energy ranks the dynamic importance of each FEM degree of freedom based on a combination of mass and modal displacement. Assuming that the target modes are mass normalized, the fractional contribution of the ith

candidate sensor to the jth modal kinetic energy is given by

$$T_{ij} = \phi_{ij}\mathbf{M}_i\boldsymbol{\varphi}_j \tag{29}$$

where ϕ_{ij}, the ith row of the jth target FEM mode shape $\mathbf{M}_i$ the ith row of the FEM mass matrix $\boldsymbol{\varphi}_j$ the jth target mode vector.

The average modal kinetic energy for each DOF is computed by forming the matrix $\mathbf{T}$ and averaging each row (over all the target modes). In practice, the DOF are typically ranked, and the most important ones retained such that approximately 90% of the modal kinetic energy is captured by the sensor set.

A.2.2. Effective/Independence (EfI)

The effective independence algorithm aims to place the sensors such that the target modes are as linearly independent as possible, which is required for the Modal TAM. The sensor placement process begins by designating a large set of candidate sensor locations from which the smaller final sensor configuration is selected. There are two approaches that can be taken. In its original form, the effective independence method iteratively reduces the large candidate set down to the desired number of sensor locations [24]. In its most recent form [25], the method starts with a small initial set of sensors and expands it to the desired number. For this work, the original form of the algorithm was used. The candidate sensor set included all translational degrees of freedom. Kammer [24] suggested that optimal sensor placement is achieved when the determinant of the Fisher Information Matrix $\mathbf{Q}$ is maximized, where

$$\mathbf{Q} = \boldsymbol{\varphi}_a^T\boldsymbol{\varphi}_a \tag{30}$$

and $\boldsymbol{\varphi}_a$ is the target mode shape matrix partitioned to the sensor degrees of freedom. Maximizing the information matrix determinant will maximize the spatial independence of the target mode partitions. It will also maximize the signal strength of the target modal responses in the sensor output, which is very desirable in the presence of noise. The effective independence of the ith degree of freedom is given by

$$E_{Di} = (\boldsymbol{\varphi}_a)_i\mathbf{Q}^{-1}(\boldsymbol{\varphi}_a)_i^T \tag{31}$$

$$0.0 \leq E_{Di} \leq 1.0 \tag{32}$$

where $(\boldsymbol{\varphi}_a)_i$ is the ith row of the target mode partition matrix, which is associated with the ith candidate sensor location. A value of zero indicates that the ith sensor contributes nothing to the linear independence of the target modes or even their observability, and a value of 1.0 indicates that the corresponding sensor is absolutely vital to the independence of the target modes and thus cannot be deleted from the candidate set.

A.2.3. Condition number sensor selection (C#)

The modal filtering process upon which the Modal TAM is based depends upon the mode shape matrix for the a-set degrees of freedom, $(\boldsymbol{\varphi}_a^T\boldsymbol{\varphi}_a)$, being invertible. If $\boldsymbol{\varphi}_a$ has a large condition number, then high sensitivity may be encountered when attempting to reconstruct the response at the omitted degrees of freedom from the response at the a-set degrees of freedom. Mayes et al. [26] proposed an algorithm that is here named the condition number sensor placement technique that places sensors to minimize the condition number of $\boldsymbol{\varphi}_a$. One would hope that this would minimize the sensitivity of the Modal TAM to errors in the measurements at the a-set degrees of freedom. Mayes suggested the following approach to obtain a sensor set that minimizes the condition number of $\boldsymbol{\varphi}_a$. One begins with an initial sensor set, typically a visualization set, of sensors that must be included in the test. Each of the other sensors is then considered one at time (or triax by triax), and the condition number of the mode shape matrix with that sensor included is computed and stored. The process is repeated for all of the candidate sensors, and the sensor that reduces the condition number of the mode shape matrix the most is retained. The process can then be repeated to add another sensor or group of sensors until the desired number of sensors is reached, or until the condition number ceases to decrease significantly. Although this process of locally-optimal steps does not guarantee that a global optimum sensor set is obtained, the method has proven very effective; Mayes has used this criterion to optimize sensor placement in another work [26], as well as in a few other unpublished applications. This sensor placement strategy, herein denoted the C# method, can be used to construct both Modal and Inverse TAMs.

References

[1] T.K. Hasselman, R.N. Coppolino, D.C. Zimmerman, Criteria for modeling accuracy: a state-of-the-practice survey, in: Proceedings of the 18th International Modal Analysis Conference, San Antonio, TX, 2000.
[2] USAF, Military Handbook 340A: Test requirements for launch, upper-stage, and space vehicles, Vol I: Baselines, (MIL-HDBK-340A), United States Air Force, 1999.
[3] NASA, NASA-STD-5002, Loads analyses of spacecraft and payloads, NASA June, 1996 1996.
[4] R.J. Guyan, Reduction of mass and stiffness matrices, *AIAA Journal* 3 (1965) 380.
[5] D.C. Kammer, B.M. Jensen, D.R. Mason, Test-analysis correlation of the space shuttle solid rocket motor center segment, *Journal of Spacecraft and Rockets* 26 (1989) 266–273.
[6] D.C. Kammer, Test-analysis model development using an exact modal reduction, *International Journal of Analytical and Experimental Modal Analysis* 2 (1987) 174–179.

[7] D.C. Kammer, A hybrid approach to test-analysis-model development for large space structures, *Journal of Vibration and Acoustics* 113 (1991) 325–332.
[8] J. O'Callahan, P. Avitable, R. Riemer, System equivalent reduction expansion process, in: Proceedings of the 7th International Modal Analysis Conference, Las Vegas, NV, 1989, pp. 29–37.
[9] J. O'Callahan, A procedure for an improved reduced system (IRS) model, in: Proceedings of the 7th International Modal Analysis Conference, Las Vegas, NV, 1989, pp. 17–21.
[10] Y.T. Chung, S. Simonian, Assessments of model correlation using dynamic reduction and static reduction, Aerospace Technology Conference, 1988.
[11] A.M. Freed, C.C. Flanigan, A comparison of test-analysis model reduction methods, in: Proceedings of the 8th International Modal Analysis Conference, Kissimmee, FL, 1990.
[12] P. Avitable, F. Pechinsky, J. O'Callahan, Study of modal vector correlation using various techniques for model reduction, in: Proceedings of the 10th International Modal Analysis Conference, San Diego, CA, 1992.
[13] T.G. Carne, C.R. Dohrmann, A modal test design strategy for model correlation, in: Proceedings of the 13th International Modal Analysis Conference, Nashville, TN, 1995.
[14] Y. Matsumura, Uncertainty in cross orthogonality checks, *JSME International Journal, Series C (Mechanical Systems, Machine Elements and Manufacturing)* 46 (2003) 692–698.
[15] D.C. Kammer, Sensor set expansion for modal vibration testing, *Mechanical Systems and Signal Processing* 19 (2005) 700–713.
[16] J.H. Gordis, An analysis of the improved reduced system (IRS) reduction procedure, in: Proceedings of the 10th International Modal Analysis Conference, San Diego, CA, 1992, pp. 471-479.
[17] P. Blelloch, H. Vold, Orthogonality and large models–what's the problem?, in: Proceedings of the 23rd International Modal Analysis Conference (IMAC XXIII) Orlando, Florida, 2005.
[18] A. Ang, W. Tang, *Probability Concepts in Engineering Planning and Design: Vol. 1-Basic Principles*, John Wiley and Sons, Inc., New York, NY, 1975.
[19] T.G. Carne, D. Todd Griffith, M.E. Casias, Support conditions for experimental modal analysis, *Sound and Vibration* 41 (2007) 10–16.
[20] P. Guillaume, P. Verboven, and S. Vanlanduit, Frequency-domain maximum likelihood identification of modal parameters with confidence intervals, in: Proceedings of the International Seminar on Modal Analysis (ISMA-23) Leuven, Belgium, 1998.
[21] P. Verboven, E. Parloo, P. Guillaume, M. V. Overmeire, Autonomous modal parameter estimation based on a statistical frequency domain maximum likelihood approach, in: Proceedings of the 19th International Modal Analysis Conference (IMAC-19) Kissimmee, Florida, 2001, pp. 1511–1517.
[22] S. Vanlanduit, P. Verboven, P. Guillaume, J. Schoukens, An automatic frequency domain modal parameter estimation algorithm, *Journal of Sound and Vibration* 265 (2003) 647–661.
[23] B.W. Silverman, *Density Estimation for Statistics and Data Analysis*, Chapman and Hall, London, 1986.
[24] D.C. Kammer, Sensor placement for on-orbit modal identification and correlation of large space structures, *Journal of Guidance Control and Dynamics* 14 (1991) 251–259.
[25] D.C. Kammer, Sensor set expansion for modal vibration testing, *Mechanical Systems and Signal Processing* 19 (2005) 700–713.
[26] R.L. Mayes, P.S. Hunter, T.W. Simmermacher, M.S. Allen, Combining experimental and analytical substructures with multiple connections, in: Proceedings of the 26th International Modal Analysis Conference (IMAC XXVI) Orlando, Florida, 2008.